Steel and Composite Structures, *Vol. 27, No. 5 (2018) 623-632*
DOI: https://doi.org/10.12989/scs.2018.27.5.623

A lateral load pattern based on energy evaluation for eccentrically braced frames

Ali Fakhraddini [a], Mohammad Javad Fadaee [*] and Hamed Saffari [b]

Department of Civil Engineering, Shahid Bahonar University of Kerman, P.O. Box 76175-133, Kerman, Iran

(*Received June 7, 2017, Revised February 10, 2018, Accepted April 3, 2018*)

Abstract. Performance-Based Plastic Design (PBPD) method has been recently developed to evaluate the behavior of structures in different performance levels. The PBPD method utilizes a base shear force and a lateral load pattern that are estimated based on energy and yielding mechanism concepts. Using of current lateral force pattern results in weak structural members in upper stories of a structure so that the values of the story drift in these stories are larger than the target drift, particularly in high-rise buildings. Therefore, such distribution requires modifications to overcome this drawback. This paper proposes a modified lateral load pattern for steel Eccentrically Braced Frames (EBFs) based on parametric study. In order to achieve the modified load pattern, a group of 26 EBFs has been analyzed under a set of 20 earthquake ground motions. Additionally, results of nonlinear dynamic analyses of EBFs have been post-processed by nonlinear regression analysis in order to derive the new load pattern. To prove the efficiency of present study, three EBFs as examples were designed by modified pattern and current PBPD distribution. Inelastic dynamic analyses results showed that the story drifts using modified lateral load pattern were well within the target values in comparison with current pattern in PBPD, particularly where the effect of the height is significant. The modified load pattern reduces the possibility of underdesigning in upper levels and overdesigning in lower levels of the frames.

Keywords: performance-based plastic design; lateral load pattern; eccentrically braced frames; energy balance; steel building

1. Introduction

Eccentrically braced frame (EBF) is a lateral load resisting system used for steel structures to resist forces induced by strong ground motions. An EBF is essentially a hybrid system which combines the stiffness of concentrically braced frames and the moment frames ductility. EBFs are expected to accommodate inelastic deformation through ductile yielding of the link when such frames are subjected to earthquake loading. The link becomes the focal point of an EBF and behaves as a structural fuse which can dissipate seismic input energy. Based on the capacity design method, other members of an EBF (including braces, columns and beams segments outside the links) are designed to remain essentially elastic. Nevertheless, plastic hinges are not developed in all stories in the EBFs that are designed based on current building codes. Thus, damage concentrates only in some of the floors (Mohammadi and Sharghi 2014, Lian *et al*. 2015, Saffari *et al*. 2017). Accordingly, Performance-Based Seismic Design (PBSD) of structure is carried out somewhat indirectly, while Performance-Based Plastic Design (PBPD) is known as a direct PBSD technique according to energy and yielding mechanism concepts. This method basically does not requires any assessment such as pushover or nonlinear dynamic analysis following the design.

The PBPD method has been previously applied to different types of structures (Lee and Goel 2001, Lee *et al*. 2004, Chao and Goel 2005, 2008, Chao *et al*. 2007, Goel *et al*. 2010, Sahoo and Chao 2010, Liao and Goel 2012, Bai and Ou 2016, Bai *et al*. 2017, Ke *et al*. 2018, Ke and Yam 2018). In PBPD method, the lateral load distribution is approximated based on an energy-balance criterion (Lee and Goel 2001, Ke and Yam 2016). Using the lateral force distribution which has been proposed in some references (Lee and Goel 2001, Chao and Goel 2005) results in having weak structural members in upper stories so that the values of story drift in these stories are greater than the target drift, particularly for medium and high-rise buildings. Therefore, this method needs to be modified to overcome such deficiency. The lateral load pattern for EBFs has been modified in this research based on parametric study which includes analyzing a group of 26 EBFs on a wide range of height under a set of 20 earthquake ground motions. Subsequently, nonlinear regression analysis is used for processing of nonlinear dynamic analysis results to derive new relation which can estimate lateral load pattern on EBFs.

In order to validate the efficiency of the new load pattern, three sample EBFs (4, 8, and 16 story) have been designed by both modified pattern and current distribution

*Corresponding author, Professor,
E-mail: mjfadaee@uk.ac.ir
[a] Ph.D., E-mail: ali.fakhreddini@eng.uk.ac.ir
[b] Professor, E-mail: hsaffari@uk.ac.ir

ISSN: 1229-9367 (Print), 1598-6233 (Online)

of PBPD. The results show an acceptable accuracy in estimation of peak inelastic drift using modified load pattern rather than current PBPD, specifically in high-rise frames.

2. Fundamentals of PBPD

A design base shear for each performance level and a lateral load distribution are two main requirements of PBPD method. In this method, after choosing yield mechanism and target drift, the design base shear is determined by equating external work due to lateral forces to internal work performed by structural elements. The design base shear can be determined as (Lee and Goel 2001)

$$\frac{V_y}{W} = \frac{-\alpha + \sqrt{\alpha^2 + 4\gamma\left(S_a / g\right)^2}}{2} \tag{1}$$

where W is the total weight of equivalent Single Degree of Freedom system (SDOF); V_y is yield base shear; g is acceleration of gravity; S_a is pseudo acceleration spectrum; γ is computed as

$$\gamma = \frac{2\mu_s - 1}{R_\mu^2} \tag{2}$$

where μ_s is structural ductility factor and R_μ is ductility reduction factor and α is dimensionless parameter calculated from the following formula

$$\alpha = h\frac{8\theta_p \pi^2}{T^2 W} \tag{3}$$

in which T is fundamental period, θ_p is plastic drift ratio and h is calculated as follows

$$h = \sum_{i=1}^{N} \lambda_i h_i \tag{4}$$

where λ_i is lateral force distribution coefficient of ith story and h_i is height of ith story from the base.

After determination of base shear force, a pattern of lateral forces is needed in PBPD which adjusts the stiffness and strength distribution along the height of the structure. Consequently, to design the frame members, plastic design method is performed to reach pre-defined yield mechanism.

As stated in the previous section, using the lateral force patterns which have been suggested in references (Lee and Goel 2001, Chao and Goel 2005), leads to weak structural members in upper stories so that the values of story drift in these stories are larger than the target drift, particularly in high-rise buildings. Therefore, such distribution requires adjustments to resolve this drawback. This study strives to improve the lateral load pattern.

3. Lateral force pattern in PBPD

In most current building codes, the design lateral force distributions are generally based on first-mode dynamic solution of lumped Multi-Degree-of-Freedom (MDOF) elastic systems. Nevertheless, buildings that are designed according to such process, experience larger deformation in inelastic range when they are subjected to seismic excitations. In order to attain the main objective of PBSD, it is essential to account for inelastic behavior of structures directly in the design procedure. Unlike the force distribution in the current codes, the lateral seismic-force pattern of PBPD is based on the maximum story shears which are estimated from nonlinear dynamic analyses under earthquake excitations. The ratio of the story shear at floor i to that at roof level, n, is called the shear distribution factor, β_i, which is determined from the following formula as stated by several references (Lee and Goel 2001, Chao and Goel 2005)

$$\beta_i = \frac{V_i}{V_n} = \left(\frac{\sum_{j=i}^{n} w_j h_j}{w_n h_n} \right)^{f(T)} \tag{5}$$

where w_j is the seismic weight at level j; h_i is the height of level i from the base; w_n is the roof weight; h_n is the roof height from the base, and $f(T)$ is a function of fundamental period; Accordingly, based on Eq. (5) the lateral force applied at the roof story, F_n, can be obtained as

$$\frac{V_1}{V_n} = \frac{V}{F_n} \quad \rightarrow \quad F_n = V\left(\frac{w_n h_n}{\sum_{j=1}^{n} w_j h_j} \right)^{f(T)} \tag{6}$$

Consequently, the lateral force applied at floor i, F_i, can also be determined as

$$F_i = \left(\beta_i - \beta_{i+1}\right)F_n \qquad when\ i = n,\ \beta_{i+1} = 0 \tag{7}$$

and $f(T)$ defined as the function of fundamental period is suggested as follows

$$f(T) = \eta T^{\psi} \tag{8}$$

In this paper, the values of parameters η and ψ is found based on parametric study and nonlinear dynamic analyses. In order to achieve this, a group of 26 EBFs on a wide range of height under a set of 20 earthquake ground motions have been selected and analyzed as explained as follows.

3.1 Framed models and ground motions considered for lateral force calculation

In this study, two groups of 2-D EBFs with single and double bracing bays have been used for parametric study whose typical configurations are shown in Fig. 1. The uniform story height and bay length are 144 in and 360, respectively. The number of stories of the frames, n_s, are shown in Table 1. Taking the link length, e, equal to aL (see Fig. 1), two values, 0.1 and 0.2, are assigned for parameter

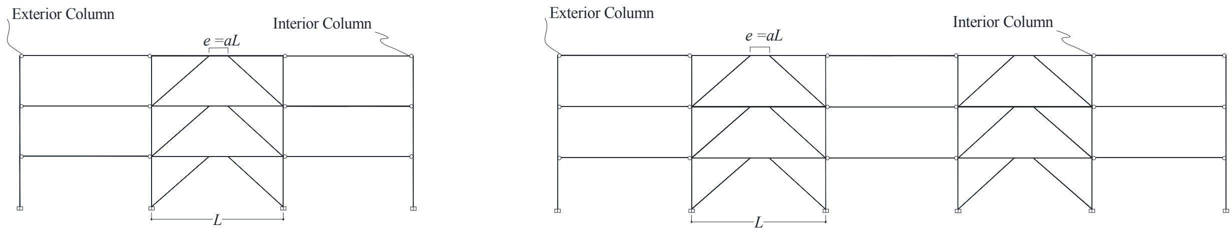

(a) Single bay EBF (b) Double bays EBFs

Fig. 1 Typical configurations of EBFs

Table 1 Section sizes of the EBFs considered in parametric study

n_s	Link length $a = e/L$	Exterior column*	Interior column*	Link beam*	Gravity beam* (all stories)	Brace **
3 Single bay	0.1	3(14x30)	3(14x132)	3(14x48)	14x109	2(6x1/2)+ 6x1/4
	0.2	3(14x30)	3(14x132)	14x53+ 2(14x48)	14x109	6x1/2+ 2(6x1/4)
6 Single bay	0.1	3(14x38)+ 3(14x38)	3(14x311)+ 3(14x132)	3(14x53)+ 3(14x48)	14x109	5(6x1/2)+ 6x1/4
	0.2	3(14x38)+ 3(14x30)	3(14x311)+ 3(14x132)	2(14x68)+ 4(14x48)	14x109	3(6x1/2)+ 3(6x1/4)
9 Single bay	0.1	3(14x48)+ 3(14x38)+ 3(14x30)	3(14x500)+ 3(14x311)+ 3(14x132)	4(14x53)+ 5(14x48)	14x109	7(6x1/2)+ 2(6x1/4)
	0.2	3(14x48)+ 3(14x38)+ 3(14x30)	3(14x500)+ 3(14x311)+ 3(14x132)	3(14x68)+ 2(14x53)+ 4(14x48)	14x109	7(6x1/2)+ 2(6x1/4)
12 Single bay	0.1	3(14x61)+ 3(14x48)+ 3(14x38)+ 3(14x30)	3(14x665)+ 3(14x500)+ 3(14x311)+ 3(14x132)	4(14x68)+ 2(14x53)+ 6(14x48)	14x109	9(6x1/2)+ 3(6x1/4)
	0.2	3(14x61)+ 3(14x48)+ 3(14x38)+ 3(14x30)	3(14x665)+ 3(14x500)+ 3(14x311)+ 3(14x132)	8(14x68)+ 4(14x48)	14x109	9(6x1/2)+ 3(6x1/4)
15 Single bay	0.1	3(14x68)+ 3(14x61)+ 3(14x48)+ 3(14x38)+ 3(14x30)	3(14x730)+ 3(14x665)+ 3(14x500)+ 3(14x311)+ 3(14x132)	8(14x68)+ 2(14x53)+ 5(14x48)	14x109	5(8x1/2)+ 8(6x1/2)+ 2(6x1/4)
	0.2	3(14x68)+ 3(14x61)+ 3(14x48)+ 3(14x38)+ 3(14x30)	3(14x730)+ 3(14x665)+ 3(14x500)+ 3(14x311)+ 3(14x132)	14x132+ 2(14x82)+ 3(14x74)+ 9(14x68)	14x109	5(8x1/2)+ 8(6x1/2)+ 2(6x1/4)
18 Single bay	0.1	6(14x68)+ 3(14x61)+ 3(14x48)+ 3(14x38)+ 3(14x30)	6(14x730)+ 6(14x665)+ 3(14x426)+ 3(14x176)	3(14x159)+ 4(14x145)+ 8(14x132)+ 14x82+ 14x74+ 14x68	14x109	9(8x1/2)+ 8(6x1/2)+ 6x1/4
	0.2	6(14x68)+ 3(14x61)+ 3(14x48)+ 3(14x38)+ 3(14x30)	6(14x730)+ 6(14x665)+ 3(14x426)+ 3(14x176)	6(14x176)+ 3(14x159)+ 3(14x145)+ 5(14x132)+ 14x68	14x109	11(8x1/2)+ 6(6x1/2)+ 6x1/4

* W-type sections; ** HSS-type sections

Table 1 Continued

n_s	Link length $a = e/L$	Exterior column*	Interior column*	Link beam*	Gravity beam* (all stories)	Brace **
3 Double bays	0.1	3(14x99)	3(14x233)	3(14x74)	14x99	12x1/2+ 2(10x1/2)
	0.2	3(14x99)	3(14x233)	3(14x82)	14x99	2(12x1/2)+ 10x1/2
5 Double bays	0.1	3(14x120)+ 2(14x99)	3(14x283)+ 2(14x233)	2(14x120)+ 3(14x82)	14x99	2(14x1/2)+ 3(12x1/2)
	0.2	4(14x120)+ 1(14x99)	3(14x283)+ 2(14x233)	3(14x120)+ 2(14x82)	14x99	3(14x1/2)+ 2(12x1/2)
7 Double bays	0.1	4(14x176)+ 3(14x120)	4(14x550)+ 3(14x283)	4(14x120)+ 3(14x82)	14x99	3(14x1/2)+ 4(12x1/2)
	0.2	4(14x176)+ 3(14x120)	4(14x550)+ 3(14x283)	5(14x120)+ 2(14x82)	14x99	5(14x1/2)+ 2(12x1/2
10 Double bays	0.1	3(14x176)+ 3(14x120)+ 3(14x68)	4(14x550)+ 3(14x311)+ 3(14x90)	5(14x120)+ 5(14x109)	14x99	6(14x1/2)+ 4(12x1/2)
	0.2	3(14x176)+ 3(14x120)+ 3(14x68	4(14x550)+ 3(14x311)+ 3(14x90	7(14x120)+ 3(14x109	14x99	8(14x1/2)+ 2(12x1/2)
12 Double bays	0.1	3(14x176)+ 3(14x120)+ 3(14x68)+ 3(14x30)	3(14x665)+ 3(14x500)+ 3(14x311)+ 3(14x132)	4(14x159)+ 2(14x120)+ 6(14x48)	14x99	4(14x5/8)+ 4(12x1/2) + 4(8x1/2)
	0.2	3(14x176)+ 3(14x120)+ 3(14x68)+ 3(14x30	3(14x665)+ 3(14x500)+ 3(14x311)+ 3(14x132)	6(14x159)+ 4(14x120)+ 2(14x48)	14x99	6(14x5/8)+ 5(12x1/2) + 1(8x1/2)
15 Double bays	0.1	3(14x233)+ 3(14x176)+ 3(14x120)+ 3(14x68)+ 3(14x30)	4(14x730)+ 3(14x665)+ 3(14x500)+ 3(14x311)+ 2(14x132)	8(14x159)+ 2(14x120)+ 5(14x48)	14x99	5(16x5/8)+ 8(12x1/2)+ 2(8x1/2)
	0.2	3(14x233)+ 3(14x176)+ 3(14x120)+ 3(14x68)+ 3(14x30	4(14x730)+ 3(14x665)+ 3(14x500)+ 3(14x311)+ 2(14x132)	10(14x159)+ 3(14x120)+ 2(14x48)	14x99	8(16x5/8)+ 5(12x1/2)+ 2(8x1/2))
18 Double bays	0.1	6(14x233)+ 3(14x176)+ 3(14x120)+ 3(14x68)+ 3(14x30)	7(14x730)+ 3(14x665)+ 3(14x500)+ 3(14x311)+ 2(14x132)	10(14x159)+ 3(14x120)+ 5(14x48)	14x99	8(16x5/8)+ 8(12x1/2)+ 2(8x1/2)
	0.2	6(14x233)+ 3(14x176)+ 3(14x120)+ 3(14x68)+ 3(14x30)	7(14x730)+ 3(14x665)+ 3(14x500)+ 3(14x311)+ 2(14x132)	12(14x159)+ 4(14x120)+ 2(14x48)	14x99	11(16x5/8) + 5(12x1/2)+ 2(8x1/2)

* W-type sections; ** HSS-type sections

a in the design phase. While all bays without EBF have simple connections, in the EBF bays, the brace-to-beam and the beam-to-column connections are fully restrained.

The uniform dead and live loads of all beams are 0.12 kips/in and 0.06, respectively. The EBFs have been designed based on plastic design method that satisfied target drift ratio criteria of 2%. All frames are assumed to be founded on firm soil, class C of NEHRP, and located in the region of the highest seismicity. The yield strength of steel is assumed as F_y = 50 ksi for all structural members. Final section sizes of all frames are summarized in Table 1. In this table, phrases such as 3(14×311) + 3(14×132) show that

Table 2 Characteristics of selected earthquake ground motions

SAC Name	Duration (sec.)	Magnitude (Mw)	Distance (km)	PGA (in/sec^2)
LA01	39.38	6.9	10.0	178.0
LA02	39.08	6.9	10.0	261.0
LA03	39.08	6.5	4.1	152.0
LA04	39.08	6.5	4.1	188.4
LA05	39.08	6.5	1.2	116.4
LA06	39.08	6.5	1.2	90.6
LA07	79.98	7.3	36.0	162.6
LA08	79.98	7.3	36.0	164.4
LA09	79.98	7.3	25.0	200.7
LA10	79.98	7.3	25.0	139.1
LA11	39.98	7.0	12.4	256.9
LA12	39.98	7.0	12.4	374.4
LA13	59.98	6.7	6.7	261.8
LA14	59.98	6.7	6.7	253.7
LA15	14.95	6.7	7.5	206.0
LA16	14.95	6.7	7.5	223.9
LA17	59.98	6.7	6.4	219.9
LA18	59.98	6.7	6.4	315.5
LA19	59.98	6.0	6.7	393.5
LA20	59.98	6.0	6.7	380.9

the first three stories possess columns with W14×311 section sizes, while the three higher stories possess columns with W14×132 section sizes.

Subsequently, twenty different earthquake ground motions corresponding to a 10% probability of exceedance in a 50-year period are considered for the nonlinear time history analysis in PERFORM-3D software (2007). These ground motions were compiled by the SAC for a site in Los Angeles, California (Somerville *et al.* 1997). The basic parameters of the records are summarized in Table 2.

One of the main requirements of nonlinear analysis is the definition of non-linear formation of plastic hinges (American Society of Civil Engineers 2013). Members of the EBFs are designed such that non-linear behavior concentrates on shear link, while other members remain linear elastic (Chao and Goel 2005, Shayanfar *et al.* 2011, Ashtari and Erfani 2016). However, it is yet probable that plastic hinges could form in the braces, or at the ends of columns and beams. The frames have analyzed by means of the PERFORM-3D computer Program (CSI 2007), which has a built-in shear link model. The strength envelopes of the shear links, beams and columns, which include degradation used for modeling are shown in Fig. 2.

3.2 Model verification

To validate the results, specimen with short link (Okazaki *et al.* 2006) is modeled by means of the PERFORM-3D computer program (CSI 2007), and the results are compared with those in experiment. The hysteretic curve of selected link test specimen from Okazaki *et al.* (2006) and pushover analysis are shown in Fig. 3. As it can be seen from this figure, pushover results of the specimen modeling in PERFORM-3D software are in a good agreement with those obtained in experiment

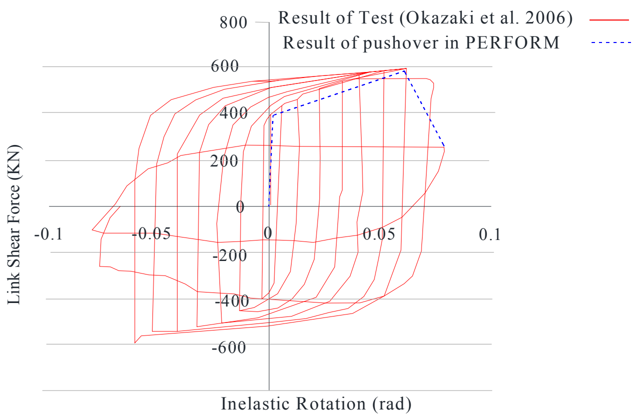

Fig. 3 Comparison of experimental results (Okazaki *et al.* 2006) and numerical modelling (PERFORM-3D, 2007)

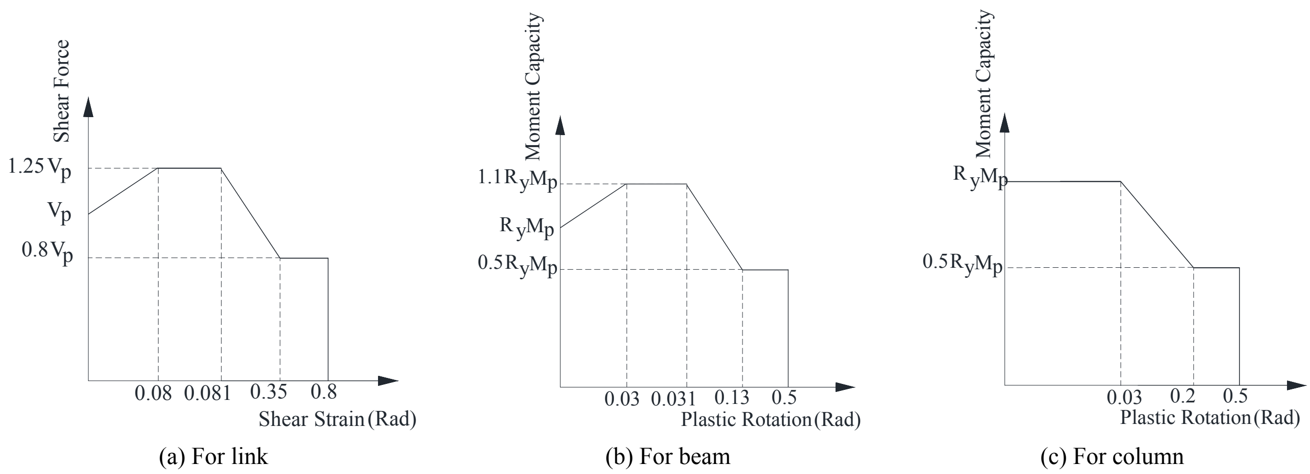

Fig. 2 Non-linear properties of EBF(Chao and Goel 2005)

3.3 Proposed load pattern

The EFs of Table 1 are analyzed to determine their response to each of the 20 seismic excitations of Table 2. The Levenberg-Marquardt algorithm of SPSS software (2013) is employed for nonlinear regression analysis based on responses of the nonlinear dynamic analyses. Consequently, the values of parameters η and ψ for establishing the modified patterns are developed as follows

$$\eta = 0.5\ ,\ \psi = -1 \quad \rightarrow \quad F_n = V\left(\frac{w_n h_n}{\sum_{j=1}^{n} w_j h_j}\right)^{1/(2T)} \tag{9}$$

The values of parameters η and ψ in Eq. (9) were previously proposed as 0.75 and -0.2, respectively by Chao and Goel (2005) based on 2 EBFs (3-story and 10-story). In this study, Eq. (9) is derived according to 26 EBFs on a wide range of height under 20 earthquake ground motion.

4. Evaluation of new load pattern

4.1 Examples

In order to validate the efficiency of new load pattern, three types of EBFs have been evaluated for sample structures. Nonlinear dynamic analyses have been performed to assess the validity of two methods, using PERFORM-3D software (2007). The EBFs selected in this study as tested frames consist of regular 4, 8, and 16-story EBFs. The configuration of these structures is the same that were studied by Speicher and Harris (2016). For all frames, the height of the first floor is 18 feet and other floor heights are 14 feet. The gravity loads are considered based on Speicher and Harris study (2016). In all frames, the brace-to-beam and the beam-to-column connections are fully restrained. All frames are assumed to be founded on firm soil class C of NEHRP and located in the region of highest seismicity. The yield strength of steel is assumed to be F_y = 50 ksi for all structural members.

These three EBFs have been designed according to both the new relation and the current lateral force distribution (Chao and Goel 2005). They have been designed based on plastic design method that satisfying target drift ratio

Table 3 Main properties of frames

Story	Bay width (ft)	Link length (in)	Floor seismic weight (kips)
4	20	30	650
8	20	30	650
16	30	39	670

Table 4 Characteristics of test earthquake records

Earthquake ground motion	Duration (sec.)	Mag. (Mw)	Dist. (km)
RSN139_TABAS_DAY-L1	21	7.35	13.94
RSN164_IMPVALL.H_H-CPE147	63.82	6.53	15.19
RSN369_COALINGA.H_H-SCN045	59.99	6.36	27.46
RSN518_PALMSPR_FVR045	20.175	6.06	14.24
RSN727_SUPER.B_B-SUP045	22.21	6.54	5.61
RSN755_LOMAP_CYC195	39.995	6.93	20.34
RSN811_LOMAP_WAH000	25.005	6.93	17.47
RSN901_BIGBEAR_BLC360	60.01	6.46	8.3
RSN1112_KOBE_OKA000	150	6.9	86.94
RSN1617_DUZCE_375-E	41.5	7.14	3.93

(a) Present study (b) Current PBPD

Fig. 4 Final properties obtained for 16-story frame

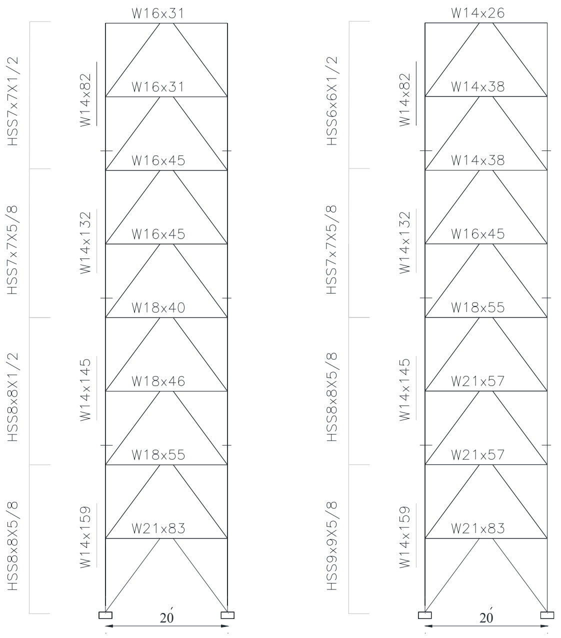

(a) Present study (b) Current PBPD

Fig. 5 Final properties obtained for 8-story frame

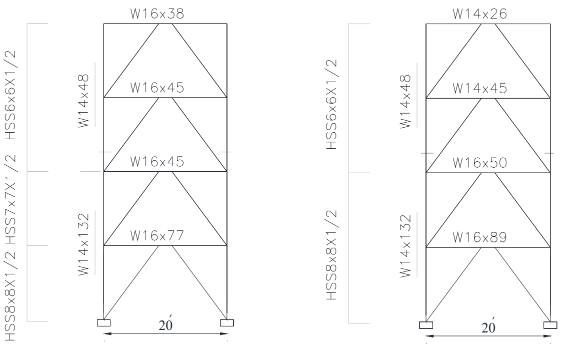

(a) Present study (b) Current PBPD

Fig. 6 Final properties obtained for 4-story frame

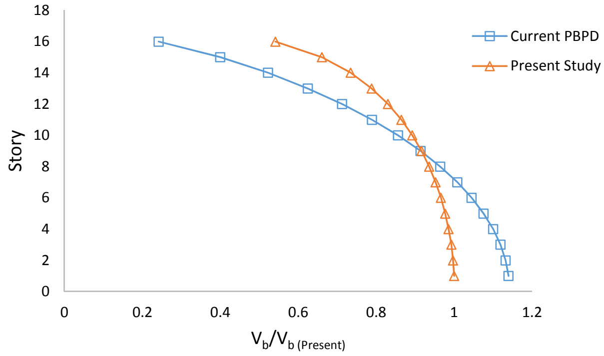

(a) 16-Story

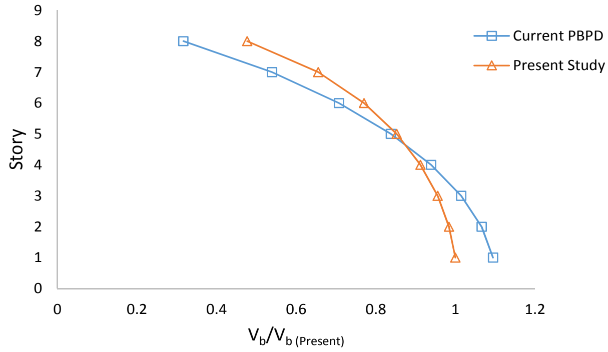

(b) 8-Story

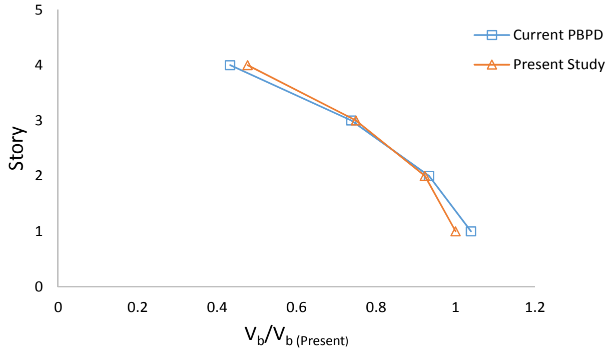

(c) 4-Story

Fig. 7 Comparison of the ratios of maximum story shears in present study and current PBPD method

criteria of 2%. Other properties of frames are listed in Table 3, and final section sizes of all frames are shown in Figs. 4 to 6. Ten earthquake ground motions are considered for the nonlinear time history analysis as test records. The basic parameters of these records are summarized in Table 4.

4.2 Results and discussion

In order to assess the new load pattern with current load pattern in PBPD (Chao and Goel 2005), some seismic parameters such as story shear and inter-story drift ratio are compared. Figs. 7(a) through 7(c) show story shears of 4, 8 and 16-story frames for two methods. As it can be seen from these figures, the story shears for present study are greater in upper floors and smaller in the lower floors in comparison with current pattern. Hence, modified load pattern provides with stronger upper stories compared to current load pattern in PBPD.

In Figs. 8 through 10, the story drift obtained by both the present study and the current pattern in PBPD for the three frames are depicted. As it can be seen, the inter-story drift in the case of 8-story and 16-story frames using the modified pattern are well within the target values in compared to current distribution in PBPD. As the effect of height is more significant in the 8-story and particularly, in the 16-story building, the modified pattern has an improved performance. In the 4-story frame, the results of modified pattern are somewhat similar to those of current distribution in PBPD.

Furthermore, Figs. 11(a) through 11(c) compare the mean story drift in frames designed by present pattern and also by current pattern in PBPD. As it can be seen, in the modified pattern, the story drifts are distributed more uniformly over the height of frames in comparison with the current pattern in PBPD. If the strength and stiffness of upper floors are increased, their story drifts will reduce. In order to make stronger upper stories, the section sizes of

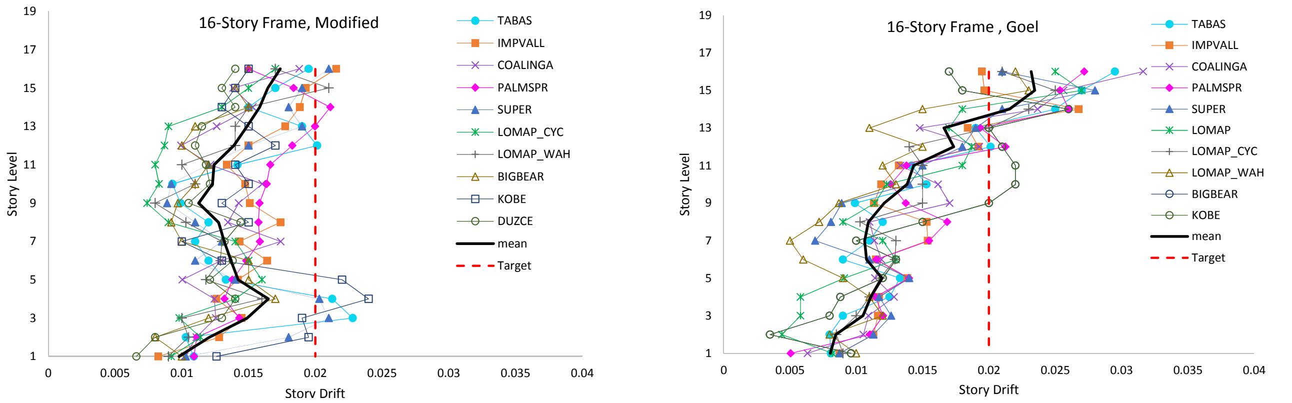

(a) Present study (b) Current PBPD

Fig. 8 Comparison of maximum story drift of 16-Story frames designed by present study and current PBPD method

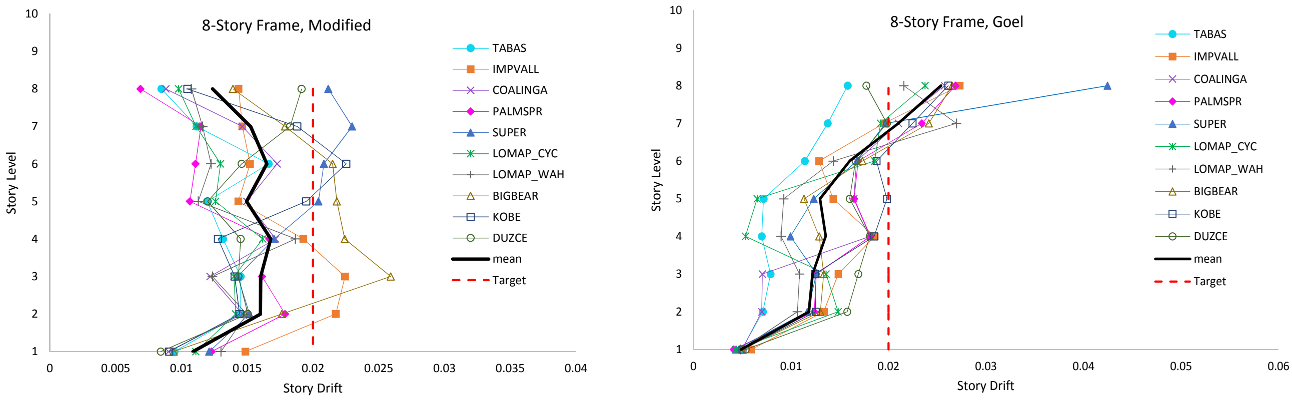

(a) Present study (b) Current PBPD

Fig. 9 Comparison of maximum story drift of 8-Story frames designed by present study and current PBPD method

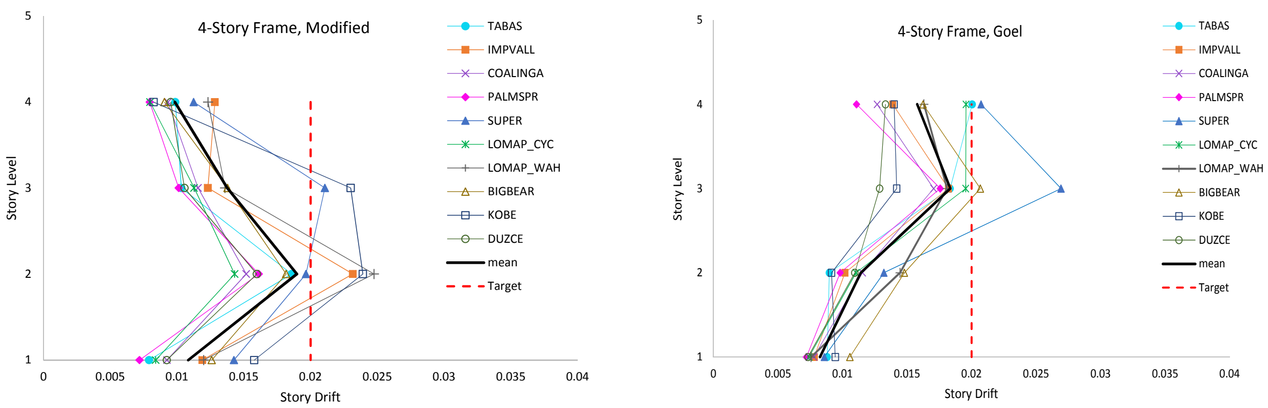

(a) Present study (b) Current PBPD

Fig. 10 Comparison of maximum story drift of 4-Story frames designed by present study and current PBPD method

upper stories must be increased; consequently, the story drifts at upper stories decrease and performance criteria will be easily satisfied.

Tables 5 through 7 show comparison of steel weights in frames for both the present study and current pattern. As shown, the total steel weights of the two frames are roughly the same. Also, in high-rise building, the frames designed by the modified pattern are slightly lighter than the frames designed by the current pattern in PBPD. Despite equality of steel in two methods, the frames designed by the present study show better performance rather than the PBPD frames with current pattern.

5. Conclusions

This research aims to modify the lateral load pattern of PBPD procedure for estimation of the seismic demand of steel EBFs subjected to seismic ground motions, particularly where the effect of the height is significant.

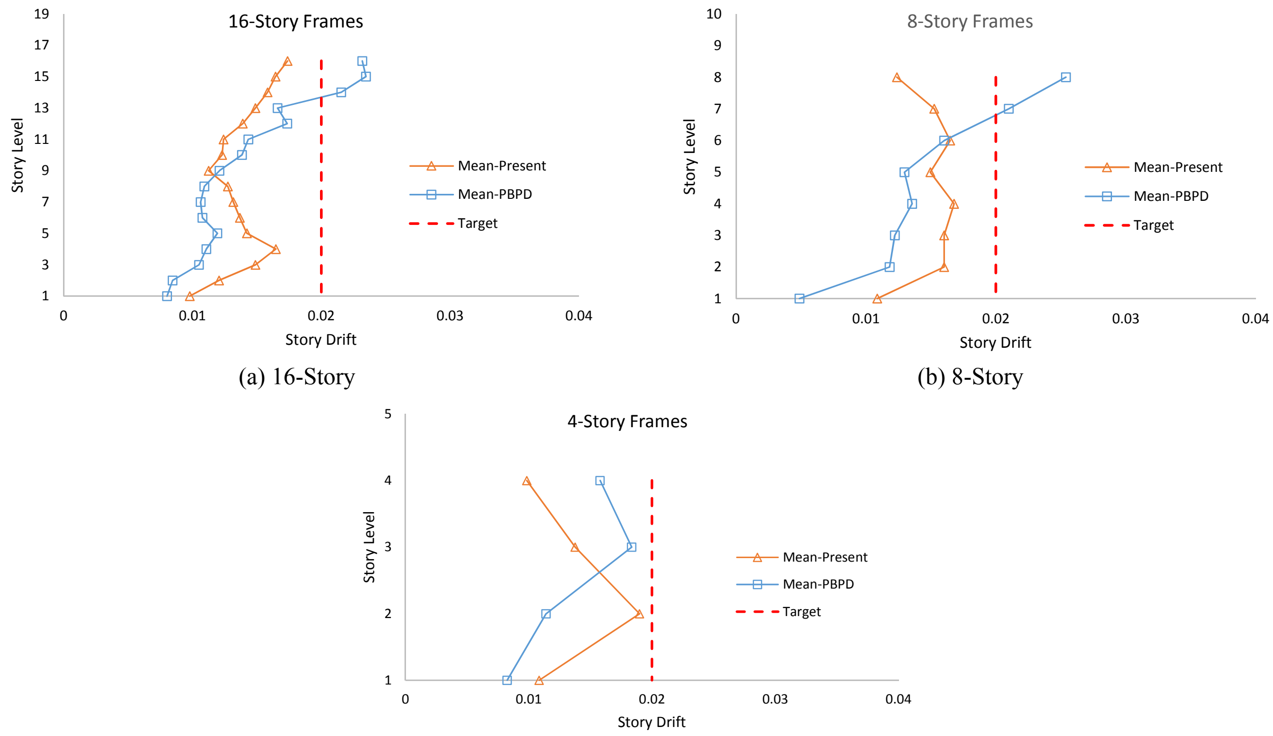

(a) 16-Story

(b) 8-Story

(c) 4-Story

Fig. 11 Comparison of mean story drift of frames designed by present study and current PBPD method

Table 5 Comparison of steel weight concerning two methods (16-story frame)

Weight calculation (kips)	Present study	Current pattern	Present study/ current pattern
Columns	138.39	181.70	0.76
Beams	35.45	28.51	1.24
Braces	61.60	59.58	1.03
Total	235.46	269.79	0.87

Table 6 Comparison of steel weight concerning two methods (8-story frame)

Weight calculation (kips)	Present study	Current pattern	Present study/ current pattern
Columns	30.21	28.08	1.07
Beams	7.05	7.47	0.94
Braces	12.74	12.17	1.04
Total	50.01	47.72	1.05

Table 7 Comparison of steel weight concerning two methods (4-story frame)

Weight calculation (kips)	Present study	Current pattern	Present study/ current pattern
Columns	10.06	10.06	1.0
Beams	3.81	3.95	0.96
Braces	4.16	5.58	0.74
Total	18.03	19.59	0.92

Thus, two groups of 2-D EBFs with single and double bracing bays have been considered and nonlinear time history analyses have been carried out under a collection of 20 ground motions. Subsequently, nonlinear regression analysis has been applied to derive modified relation which can estimate the lateral load pattern for EBFs.

Three EBFs with different height were utilized as test frames which have been designed based on modified load pattern and current PBPD distribution. Results of inelastic dynamic analyses show that the upper story drifts in the proposed method become quite smaller compared with the frames designed by means of the current pattern in PBPD, while the steel weight of two methods is approximately the same. Furthermore, the story drift pattern matches much better with the target drift limit in the frames designed by means of the proposed method and also tends to be more uniform over the height of the frames. In summary, the modified load pattern attempts to reduce the possibility of underdesigning in upper levels and overdesigning in lower levels of the frames, especially in medium and high-rise EBFs.

References

American Society of Civil Engineers, ASCE/SEI 41 (2013), Seismic evaluation and retrofit of existing buildings, Reston, VA, USA.

Ashtari, A. and Erfani, S. (2016), "An analytical model for shear links in eccentrically braced frames", *Steel Compos. Struct., Int. J.*, **22**(3), 627-645.

Bai, J. and Ou, J. (2016), "Earthquake-resistant design of buckling-restrained braced RC moment frames using performance-based plastic design method", *Eng. Struct.*, **107**,

66-79.
Bai, J., Yang, T.Y. and Ou, J. (2017), "Improved performance-based plastic design for RC moment resisting frames: development and a comparative case study", *Int. J. Str. Stab. Dyn.*, 18500505.
Chao, S.H. and Goel, S.C. (2005), "Performance-based seismic design of EBF using target drift and yield mechanism as performance criteria", Research Report UMCEE 05-05; Department of Civil and Environmental Engineering -The University of Michigan, College of Engineering, Ann Arbor-MI 48109-2125.
Chao, S.H. and Goel, S.C. (2008), "Performance-based plastic design of special truss moment frames", *AISC*, *Eng. J.* (2nd Quarter), 127-150.
Chao, S.H., Goel, S.C. and Lee, S.S. (2007), "A seismic design lateral force distribution based on inelastic state of structures", *Earthq. Spectra*, **23**(3), 547-569.
CSI (2007), PERFORM-3D v.4.0 User Manual; Computers & Structures Inc., Berkeley, CA, USA.
Goel, S.C., Liao, W.C., Bayat, M.R. and Chao, S.H. (2010), "Performance-based plastic design (PBPD) method for earthquake-resistant structures: An overview", *Struct. Des. Tall Special Build.*, **19**(1-2), 115-137.
IBM Corp. Released, IBM SPSS Statistics for Windows (2013), Version 22.0.; IBM Corp., Armonk, NY, USA.
Ke, K. and Yam, M.C.H. (2016), "Energy-factor-based damage-control evaluation of steel MRF systems with fuses", *Steel Compos. Struct.*, *Int. J.*, **22**(3), 589-611.
Ke, K. and Yam, M.C.H. (2018), "A performance-based damage-control design procedure of hybrid steel MRFs with EDBs", *J. Constr. Steel Res.*, **143**, 46-61.
Ke, K., Zhao, Q., Yam, M.C.H. and Ke, S. (2018), "Energy factors of trilinear SDOF systems representing damage-control buildings with energy dissipation fuses subjected to near-fault earthquakes", *Soil Dyn. Earthq. Eng.*, **107**, 20-34.
Lee, S.S. and Goel, S.C. (2001), "Performance-based design of steel moment frames using target drift and yield mechanism", Research Report UMCEE 01-07; University of Michigan, Ann Arbor, MI, USA.
Lee, S.S., Goel, S.C. and Chao, S.H. (2004), "Performance-based design of steel moment frames using target drift and yield mechanism", *Proceedings of the 13th World Conference on Earthquake Engineering*, Paper No. 266, Vancouver, BC, Canada.
Lian, M., Su, M. and Guo, Y. (2015), "Seismic performance of eccentrically braced frames with high strength steel combination", *Steel Compos. Struct.*, *Int. J.*, **18**(6), 1517-1539.
Liao, W.C. and Goel, S.C. (2012), "Performance Based Plastic Design and Energy Based Evaluation of Seismic Resistant RC Moment Frame", *J. Mar. Sci. Tech.*, **20**(3), 304-310.
Mohammadi, R.K. and Sharghi, A.H. (2014), "On the optimum performance-based design of eccentrically braced frames", *Steel Compos. Struct.*, *Int. J.*, **16**(4), 357-374.
Okazaki, T., Engelhardt, M.D., Nakashima, M. and Suita, K (2006), "Experimental performance of link-to-column connections in eccentrically braced frames", *J. Struct. Eng.*, **132**(8), 1201-1212.
SAC Joint Venture (1997), Develop suites of time histories, Project Task: 5.4.1; Draft Report, March 21, Sacramento, CA, USA.
Saffari, H., Damroodi, M. and Fakhraddini, A. (2017), "Assessment of seismic performance of eccentrically braced frame with vertical members", *Asian J. Civil Eng.*, **18**(2), 255-269.
Sahoo, D.R. and Chao, S.H. (2010), "Performance-based plastic design method for buckling-restrained braced frames", *Eng. Struct.*, **32**(9), 2950-2958.
Shayanfar, M.A., Barkhordari, M.A. and Rezaeian A.R. (2011), "Experimental study of cyclic behavior of composite vertical shear link in eccentrically braced frames", *Steel Compos. Struct.*, *Int. J.*, **12**(1), 13-29.
Somerville, P., Smith, N., Punyamurthula, S. and Sun, J. (1997), "Development of ground motion time histories for phase 2 of the FEMA/SAC steel project", Report No. SAC/BD-97/04; SAC Joint Venture, Sacramento, CA, USA.
Speicher, M.S. and Harris III, J.L. (2016), "Collapse prevention seismic performance assessment of new eccentrically braced frames using ASCE 41", *Eng. Struct.*, **117**, 344-357.

CC